New Journal of Physics
The open access journal at the forefront of physics

Deutsche Physikalische Gesellschaft DPG IOP Institute of Physics

OPEN ACCESS

Dynamics of dust grains in an electron–dust plasma induced by solar radiation under microgravity conditions

To cite this article: V E Fortov *et al* 2003 *New J. Phys.* **5** 102

View the article online for updates and enhancements.

You may also like

- Drag-shield drop tower residual acceleration optimisation
A Figueroa, F Sorribes-Palmer, M Fernandez De Pierola et al.
- Hetero-cellular prototyping by synchronized multi-material bioprinting for rotary cell culture system
Jessica Snyder, Ae Rin Son, Qudus Hamid et al.
- Microgravity facilities for cold atom experiments
Matthias Raudonis, Albert Roura, Matthias Meister et al.

This content was downloaded from IP address 194.95.157.36 on 27/01/2025 at 08:41

New Journal of Physics
An Institute of Physics and Deutsche Physikalische Gesellschaft Journal

Dynamics of dust grains in an electron–dust plasma induced by solar radiation under microgravity conditions

V E Fortov[1], A P Nefedov[1], O S Vaulina[1], O F Petrov[1], I E Dranzhevski[1], A M Lipaev[1] and Yu P Semenov[2]

[1] Institute for High Energy Densities, Russian Academy of Sciences, Izhorskaya 13/19, 127412, Moscow, Russia

[2] Russian Space Corporation 'Energiya', Korolev, Moscow oblast, 141070, Russia

E-mail: idranzh@ihed.ras.ru

New Journal of Physics **5** (2003) 102.1–102.17 (http://www.njp.org/)
Received 25 February 2003, in final form 11 June 2003
Published 30 July 2003

Abstract. In this paper the results of experimental investigation of the dynamic behaviour of macroparticles charged via photoemission are presented. The experimental data have been obtained for bronze particles subjected to solar radiation under conditions of microgravity (on board the Mir space station). The distribution of velocity, temperatures and charge, as well as the friction coefficient and diffusion constants, have been found. The analysis of the results obtained has shown that the polarization effects of opposite charges may appreciably influence the transport processes in a two-component electron–dust plasma, consisting of positively charged dust and emitted electrons.

PII: S1367-2630(03)59982-7
© IOP Publishing Ltd and Deutsche Physikalische Gesellschaft

Contents

1. Introduction

The dusty plasma is an ionized gas containing micron-sized charged condensed grains (dust). The combined action of the interaction between dust grains and dissipative processes in a dusty plasma can lead to the formation of both steady-state dusty structures (similar to fluids or solids) and complex dynamic configurations associated with large-scale transport processes [1]–[10]. The plasma-dust structures play an important role in the processes occurring in the upper atmosphere, where the main ionization agents are cosmic rays and solar radiation [11]–[13]. Under these conditions, the charging of atmospheric aerosols is governed by two competing processes: the absorption of atmospheric ions and electrons by grains, and the emission of electrons from the grain surface. Under the action of intense solar radiation, the grains are mainly charged via photoemission. Micron-sized grains can acquire a positive charge of 10^2–10^5 elementary charges, which can result in the formation of ordered structures [6, 14]. Moreover, the emission processes make possible the existence of two-component systems consisting of positively charged grains and the electrons emitted by them. Recently, experimental studies of dusty plasmas under microgravity conditions have attracted great attention [6]–[10]. These experiments allow one to investigate various phenomena (the charging of atmospheric aerosols and the dynamics of large dust grains $\sim$100 μm in size) that cannot be studied on the Earth [6]–[8].

The main process responsible for the dust mass transfer is diffusion, which determines the dynamic characteristics of dust systems (the phase state, wave propagation conditions, and formation of dust instabilities) and governs energy losses (dissipation) in them. Both the dust grains suspended in the buffer gas and the gas molecules or charged plasma particles can undergo diffusion (Brownian motion, self-diffusion). The transport properties of a plasma-dust cloud consisting of charged dust grains, ions and electrons can be significantly affected by the concurrent diffusion of the oppositely charged particles (ambipolar diffusion). A simple case of ambipolar diffusion in the absence of a magnetic field was investigated by Schottky (1924). However, direct experimental observations of this phenomenon without attendant processes, such as ionization or vortex currents under the Earth's gravity conditions, are missing at the present time.

The first results on the polarization effects related to the separation of opposite charges in a two-component system consisting of dust grains and photoelectrons under microgravity conditions are presented in [7]. Most experimental methods for determining the diffusion coefficients of ions and electrons are based on indirect measurements of the particle mobilities in an external electric field [15]. However, these methods introduce significant perturbations in the system under study and hence are inappropriate to diagnose particles in a plasma. In order to determine the transport properties of dust grains, spectroscopy and photon correlation methods are traditionally used. The range of applicability of these methods is limited by the short-range ordering related to the interaction between grains [16]. The methods rely on different hydrodynamic models; thus, the main problem is to determine the conditions under which these models are applicable.

The dusty plasma is a good object for experimentally studying transport phenomena in a system of interacting particles because the behaviour of dust grains can be captured by a video camera, which greatly simplifies the use of direct and indirect diagnostic methods. A weakly ionized dusty plasma can be regarded as a dissipative system of grains with the Yukawa interaction potential $\varphi = eZ_p \exp(-r/\lambda)/r$, where eZ_p is the dust grain charge, λ is the screening length, and r is the intergrain distance. The correlation between grains is governed by the dimensionless coupling parameter $\Gamma_n = (1 + \kappa + \kappa^2/2)\exp(-\kappa)\Gamma$, where $\Gamma = (eZ)^2 n_p^{1/3}/T_p$, T_p is the kinetic temperature of the grains in energy units, n_p is their number density, and $\kappa = n_p^{-1/3}/\lambda$. Numerical simulations show that, at $\Gamma_n > 1$, short-range ordering arises in Yukawa systems, the critical value of the coupling parameter Γ_n at the melting point being close to 106 [17, 18].

In this paper, we report the results of the first experiments on the grain dynamics in a dusty plasma initiated by solar radiation under microgravity conditions. The experiments were performed on board the Mir space station. The photoemission charge, velocity distribution, and friction and diffusion coefficients of dust grains, as well as the coupling parameter of the dust system, are determined. The polarization effects related to the separation of opposite charges in a two-component system consisting of positively charged dust grains and the electrons emitted by them are observed.

2. Experimental setup

A schematic of the experimental facility is shown in figure 1. The main component of the working chamber was a glass ampoule containing bronze grains (with average radius $a = 37.5\ \mu$m) coated with caesium (with a work function of $W = 1.5$ eV). The grains resided in a buffer gas (neon) at a pressure of $P = 40$ Torr. The ampoule was a cylinder, one end of which was a flat uviol window for illuminating the grains with solar radiation (figure 2). The ampoule was located near a quartz illuminator on the Mir space station under the action of intensive solar radiation. The grains in the ampoule were further illuminated with a laser beam ('laser knife') with a thickness of $\sim$500 μm. For this purpose, a 0.67 μm-diode laser was used. The image recorded with a CCD video camera was stored on a magnetic tape (with a frame frequency of 25 s^{-1}). The presence of intense solar radiation in the viewing field of the CCD camera determines the experimental field of view (i.e. all the illuminated dust particles were registered). The viewing field of the camera was a rectangle 8 mm $\times$ 9 mm in size. The camera was focused on the axis of the cylindrical ampoule. The depth of focus (at a chosen iris value of 16) was $\sim$9 mm (see figure 2). The video recording was treated with a special computer code enabling the identification of the displacement of individual grains in the viewing field of the video camera. It should be noted

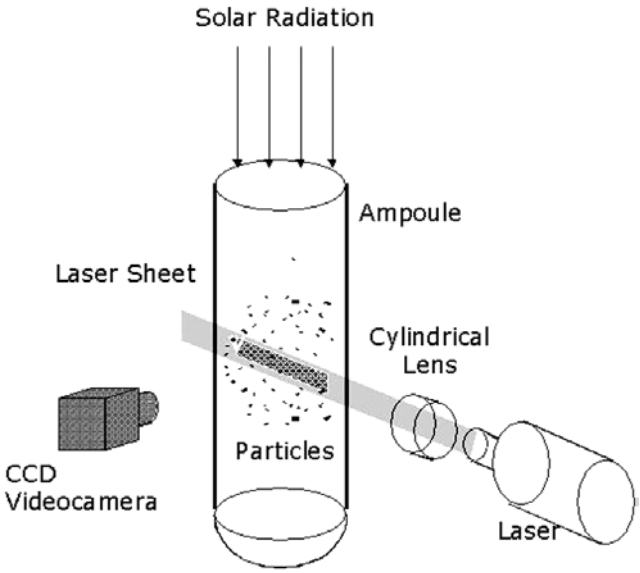

Figure 1. Schematic of the experimental facility.

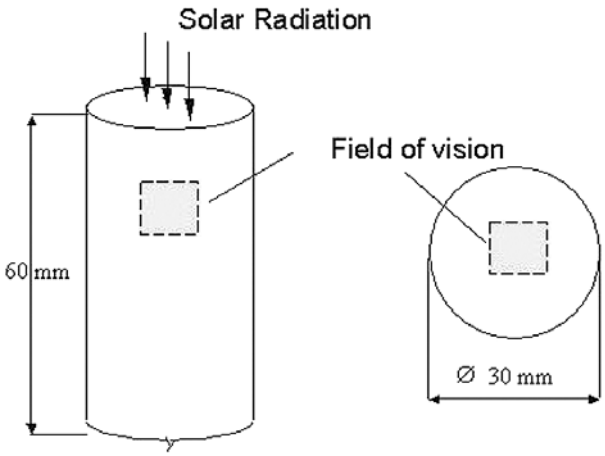

Figure 2. The geometry of the glass ampoule.

that the intensity of solar radiation is comparable with the intensity of the laser diode radiation. As a result, the number of observed grains was determined by the depth of focus of the video system, which allowed one to monitor the grain positions over a time $t > 5\nu_{\mathrm{fr}}^{-1}$, long enough to analyse the transport properties of the system (here ν_{fr} is the friction coefficient, determined by the collision frequency of the dust grains with the buffer gas molecules).

3. Description of experiment

In the first stage of the experiment, the grain behaviour under microgravity conditions in the absence of solar radiation (the 'dark' regime) was investigated. The aim of the experiment was to evaluate the characteristic time it takes for the grains to lose the velocity acquired by initially

shaking the ampoule. Since direct measurements of the damping rate of the initial perturbations in the sheet of the laser beam were unfeasible, the grain dynamics was analysed by measuring the dependence of the grain number density n_p (determined by the number of grains inside the laser sheet) on time t. These measurements showed that 2–4 s after shaking the ampoule, the grain density n_p sharply decreased from $\sim 10^3$ to $\sim$200–350 cm^{-3}. One can assume that the fast loss of grains is related to their deposition onto the ampoule wall due to the high adhesion coefficient. Then, for the time $\sim$20 min, the registered number of grains changed only slightly ($n_p \approx$ constant).

In the second stage of the experiment, the shaken ampoule was exposed to solar radiation. During the first 10 s, the grain density remained almost equal to the initial density $n_p^0 = n_p(0) \sim 900$ cm^{-3}. The time it took for the grains to depart to the ampoule wall was $\sim$5 min. Comparing with the 'dark' regime, it is reasonable to assume that the electric field arising from the irradiation of the system somehow impedes the grain adhesion on the ampoule wall. The time behaviour of the grain velocity V after the dynamic action on the system is shown in figure 3 for different regions of the viewing field. It can be seen that, over a time $t \approx$ 5–10 s after the dynamic action, the grains are involved in vibrational motion with a frequency of $\omega \sim$ 4.5–5.2 s^{-1} (a period of $\sim$1.2–1.4 s) against the background of their translational motion toward the wall.

In the third stage of the experiment, the dynamics of grains under the action of solar radiation was investigated. Initially, the bronze grains resided on the ampoule wall; hence, the experiments were carried out as follows:

(1) dynamic action (kick) upon the system at the closed porthole curtain;
(2) ageing in darkness for a time $t \approx 4\ \text{s} \gg \nu_{fr}^{-1}$ in order to reduce the grain velocities acquired with the initial kick;
(3) exposure to solar radiation; and
(4) the relaxation of grains to the initial state (return to the wall), after which the porthole curtain was closed again.

This procedure was repeated several times. The kinetic temperature and the degree of correlation of the dust grains increased for the first 3–5 s after the onset of solar illumination. The pair correlation functions for the illuminated dust cloud obtained by exclusion of the intergrain distances shorter than $l_p/2$ (where $el_p = n_p^{-1/3}$), are shown in figure 4. Although these functions cannot be used for the quantitative analysis of the degree of grain correlation in a dusty structure, they reflect qualitative changes in the system under study.

In the initial stage of illumination, the grain velocities are randomly directed. Then, 1–3 s after the onset of illumination, the grain motion acquired a directed motion towards the ampoule wall. The time of the grain migration to the ampoule wall is 3–4 min, which is nearly five orders of magnitude shorter than the characteristic time of the total diffusion losses due to Brownian motion at room temperature. The grain parameters measured at the instant $\sim$5 s after the onset of illumination are shown in figures 5–9. Figure 5 shows the trajectories of 40 grains, and (figure 6) demonstrates the time behaviour of the relative grain density $n_p(t)/n_0$. The initial grain density $n_p^0 = n_p(0)$ varied in the range 195–300 cm^{-3}, which corresponded to the results obtained in the first stage of the experiment. The spatial distributions of the drift and thermal grain velocities, the velocity distributions of dust grains, and the self-diffusion coefficients during the first 10–15 s of the experiment are shown in figures 7–9. An analysis of the experimental results is presented in the next section; it is mainly based on the data from the third stage of experiments, which were repeated several times and demonstrate the necessary repeatability.

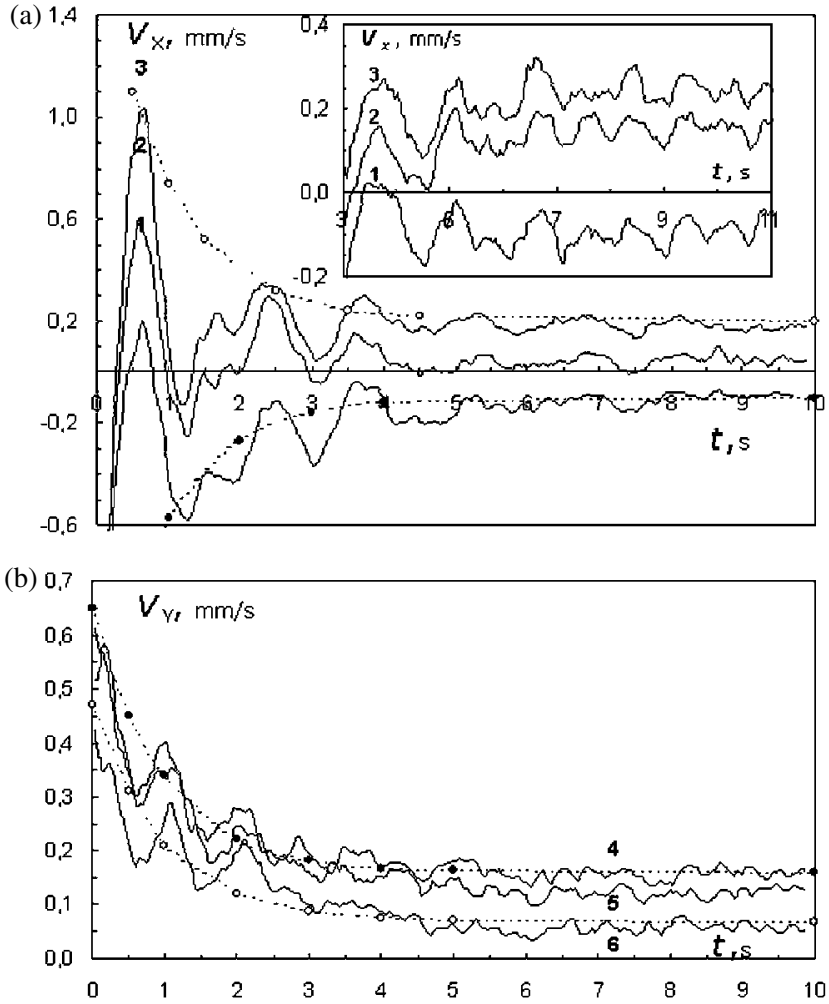

Figure 3. Grain velocities V_x and V_y along (a) the X-axis and (b) the Y-axis versus time for different viewing-field sections: $x =$ (1) 0–1, (2) 4–5, and (3) 7–8 mm at $y = 0$–8 mm and $y =$ (4) 0–1, (5) 1–2, and (6) 6–7 mm at $x = 0$–9 mm. The dashed curve shows the approximation $V(t) = V(0)\exp(-\tau_{\mathrm{Maxw}}t)$, and $\tau_{\mathrm{Maxw}} = 1\ \mathrm{s}^{-1}$.

4. Results and discussion

4.1. Temperature and velocity distribution of dust grains

Irregular variations in the magnitude and direction of the velocities of individual grains against the background of their general drift motion (see figure 5) can be associated with the grain kinetic temperature, which in the case of Maxwellian distribution over the velocities V_x and V_y, can be expressed as

$$T_{x(y)} = m_{\mathrm{p}}(\langle V_{x(y)}^2\rangle - \langle V_{x(y)}\rangle^2), \tag{1}$$

where the angular brackets stand for averaging over the ensemble and time. During the first 10–15 s, the spatial distributions of the mean (drift) velocities $\langle V_{x(y)}\rangle$ of dust grains toward the

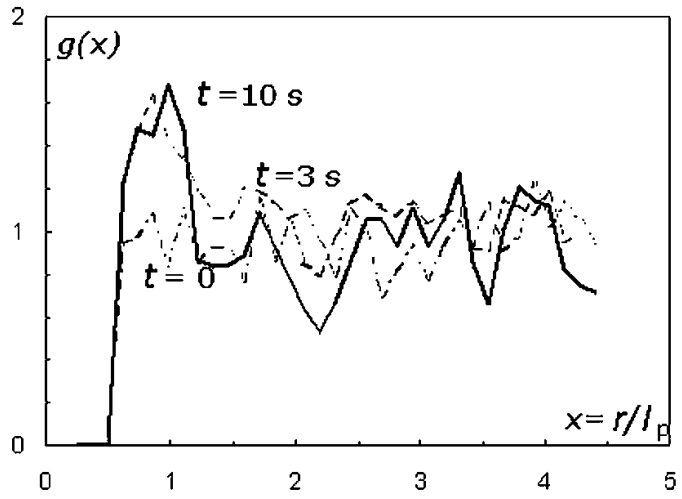

Figure 4. Pair correlation functions g ($x = r/l_p$) for an illuminated dust cloud at different times.

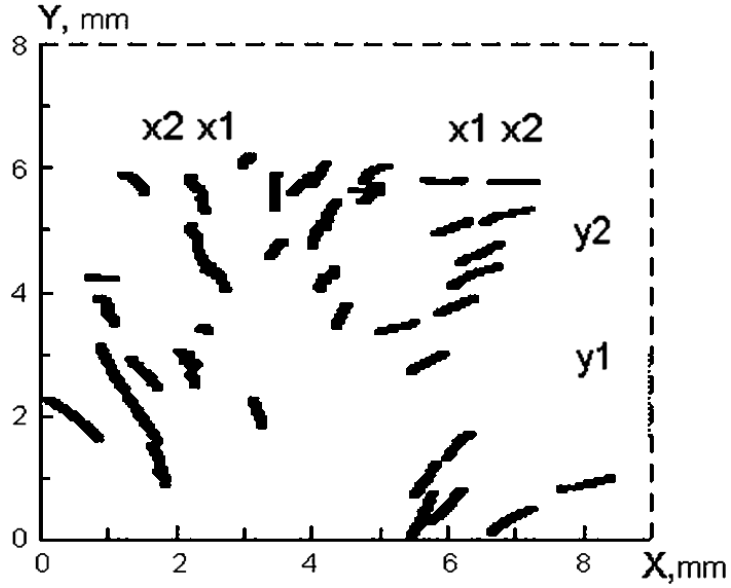

Figure 5. Particle trajectories after irradiation.

ampoule wall and the thermal velocities $V^{T}_{x(y)} = (\langle V^2_{x(y)}\rangle - \langle V_{x(y)}\rangle^2)^{1/2}$ changed only slightly (see figure 7). The recorded grain distributions over the V_x and V_y velocity components turned out to be close to Maxwellian with the temperatures calculated by formula (1) (see figure 8). At $n^0_p = 195$–300 cm^{-3}, the temperatures obtained by formula (1) for different regions of the ampoule are $T_x \cong (51\pm5)$ eV, $T_y \cong (22\pm2)$ eV; i.e., they are much higher than room temperature $T \cong 0.03$ eV. We note that the kinetic energy of random grain motion in the plasma can be non-uniformly distributed over the degrees of freedom (i.e., Maxwellian distributions with $T_x \neq T_y$ can occur) and the kinetic grain temperature can substantially exceed the temperature of the surrounding gas. These effects can be related, e.g., to the grain charge fluctuations or the spatial inhomogeneity of the plasma-dust system [3], [19]–[21]. The anomalous heating of grains has been repeatedly observed in experiments on dusty structures in laboratory plasmas [3], [21]–[23].

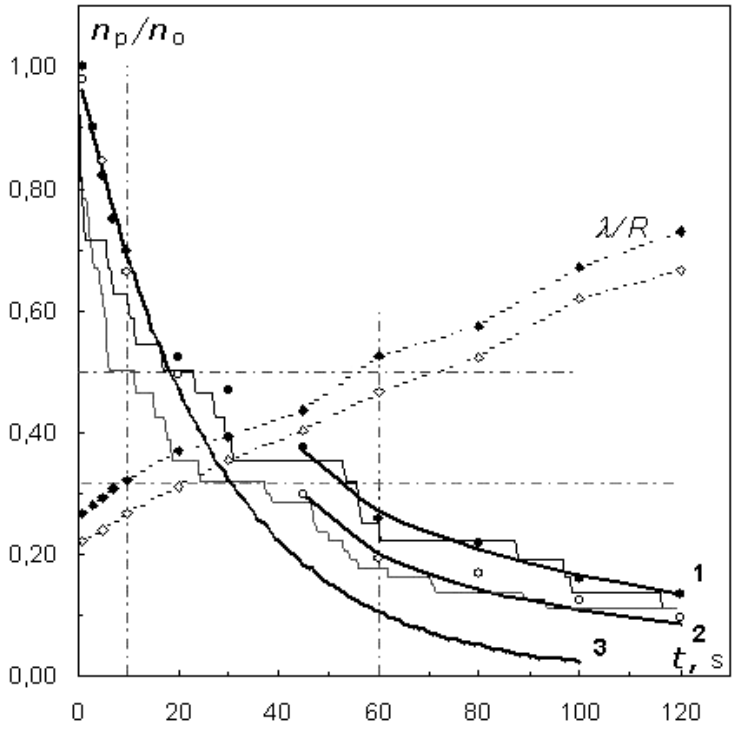

Figure 6. Measured time dependences of the relative density n_p/n_p^0 for $n_p^0 = 195$ and 300 cm^{-3} (●, ○). The light curves show the calculations by method of molecular dynamics, curves 1 and 2 correspond to approximation (15), and curve 3 shows the function $n_p/n_p^0 = \exp(-\nu_d t)$. The (♦) and (◊) show the time behaviour of λ/R for $n_p^0 = 195$ and 300 cm^{-3} respectively.

4.2. Friction coefficient and thermal diffusion coefficient

In the system under study, the grains reside in a viscous medium; hence, dissipation due to collisions with the buffer gas atoms significantly affects the grain motion. At room temperature, the mean free path of neon atoms is determined by the relationship l_n (μm/Torr) $\approx 50/P$ (Torr) [15] and, under our experimental conditions ($P = 40$ Torr) it is $l_n \approx 1.25$ μm, which is much less than the minimum radius of the bronze grains ($a_p = 25$ μm). In this case ($a_p \gg l$), the friction coefficient ν_{fr} can be written in the Stokes' approximation [24]

$$\nu_{fr} = 6\pi\eta a/m_p \equiv 4.5\eta(\rho a_p^2)^{-1}, \tag{2}$$

where ρ is the mass density of the grain and $\eta \sim 10^{-4}$ g cm^{-1} s^{-1} is the viscosity of neon at room temperature. Thus, for bronze grains with a mean radius $\langle a_p \rangle = 37.5$ μm, we have $\nu_{fr} \approx 4$ s^{-1}.

The diffusion coefficient of the non-interacting (Brownian) grains can be calculated by the measured grain temperature as

$$D_0^{x(y)} = T_p^{x(y)}/\nu_{fr} m_p. \tag{3}$$

Then, for $\nu_{fr} = 4$ s^{-1}, $T_x \cong 51$ eV, $T_y \cong 22$ eV we have $D_0^x \cong 10^{-5}$ cm^2 s^{-1} and $D_0^y \cong 4.4 \times 10^{-6}$ cm^2 s^{-1}. The grain thermal diffusion coefficients $D_p^{x(y)}$ can be directly

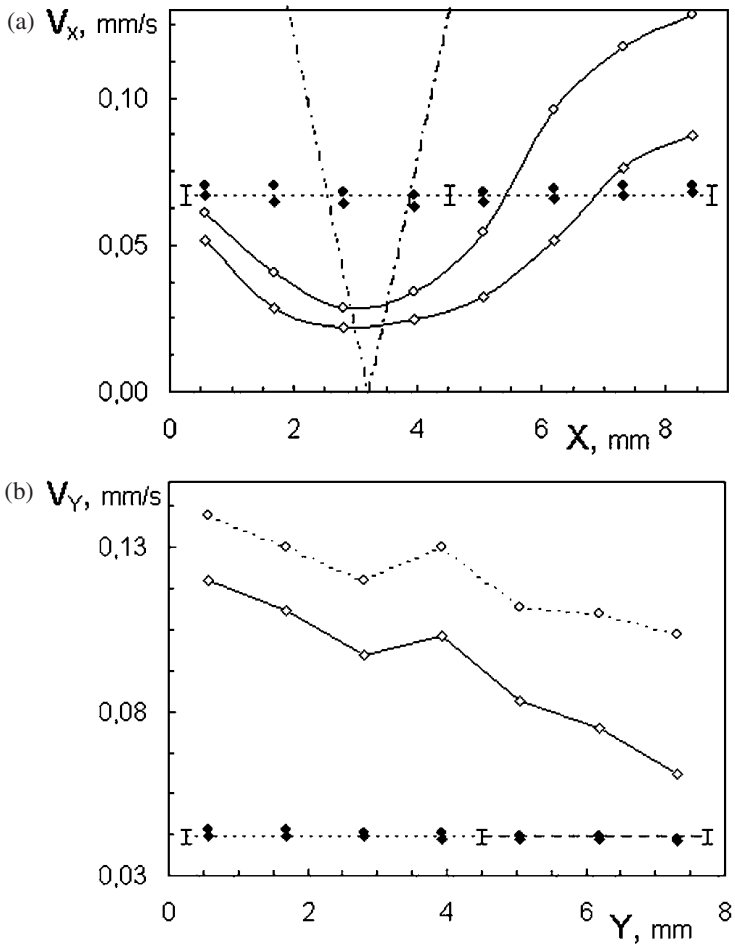

Figure 7. Spatial distributions of the drift velocity $\langle V \rangle$ (◇, ○) and thermal velocity V^{T} (◆, ●) of dust grains over (a) the X- and (b) Y-axes for $n_{\mathrm{p}}^0 = 195$ and 300 cm^{-3}. The dashed-and-dotted curve shows the minimum radial grain velocity for a dust cloud transparent to the emitted electrons.

determined from the experimental data, taking into account the regular grain drift velocities $\langle V_{x(y)} \rangle$ (see section 4.1):

$$D_{\mathrm{p}}^{x(y)}(t) = \{\langle \Delta r(t)^2 \rangle - (\langle V_{x(y)}(t) \rangle)^2\}/2t, \tag{4}$$

where $\langle \Delta r(t)^2 \rangle$ is the mean square displacement of an individual grain along either the OX (or the OY) axis. When the interaction between grains is negligible, the self-diffusion coefficient $D_{\mathrm{p}}^{x(y)}$ at $t \to \infty$ should obey the Einstein relation (3); i.e., $D_{\mathrm{p}}^{x(y)}$ $(t \to \infty) = D_0^{x(y)}$. Figure 9 illustrates the dependences $D_{\mathrm{p}}^{x(y)}(t)$ measured in some regions of the ampoule and the results of averaging these dependences over all the experiments. At $t = 4$ s, the measured $D_{\mathrm{p}}^{x(y)}(t)$ values are equal to $D_{\mathrm{p}}^{x} \approx 1.3 \times 10^{-5}$ cm^2 s^{-1} and $D_{+}^{y} \cong 5.7 \times 10^{-6}$ cm^2 s^{-1}; i.e., they are ∼30% higher than those obtained by equation (3). We note that the value $\nu_{\mathrm{fr}} \approx 4$ s^{-1}, obtained for the grain mean radius $\langle a_{\mathrm{p}} \rangle = 37.5$ μm, may not correspond to the effective friction coefficient for a polydisperse dusty system. We also note that, in the preliminary 'dark' regime, the probability for a grain departure to the wall is higher for smaller and hence more mobile grains.

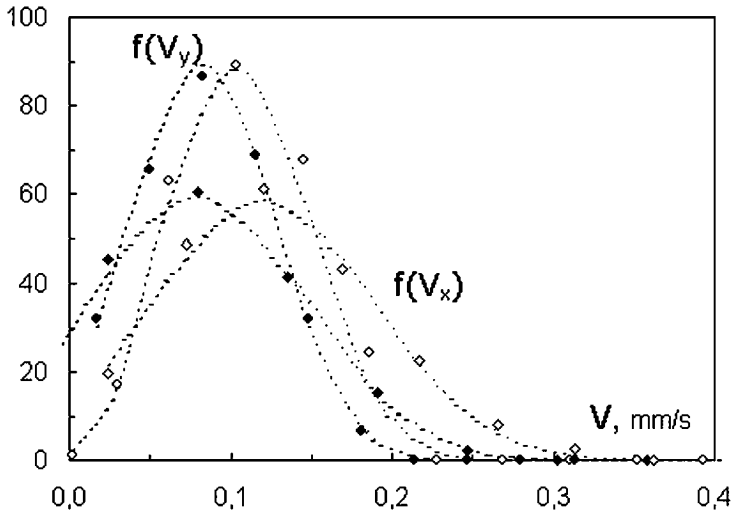

Figure 8. Particle distributions over the V_x velocity component (♦, ◊) in the region (x = 7–8 mm, y = 0–8 mm) and the V_y velocity component (●, ○) in the region (y = 5–6 mm, x = 0–9 mm) for n_p^0 = 195 (♦, ●) and 300 cm^{-3} (◊, ○). The dashed curves show the approximation of the experimental data by Maxwellian distributions with temperatures $T_x \cong 51$ eV and $T_y \cong 22$ eV.

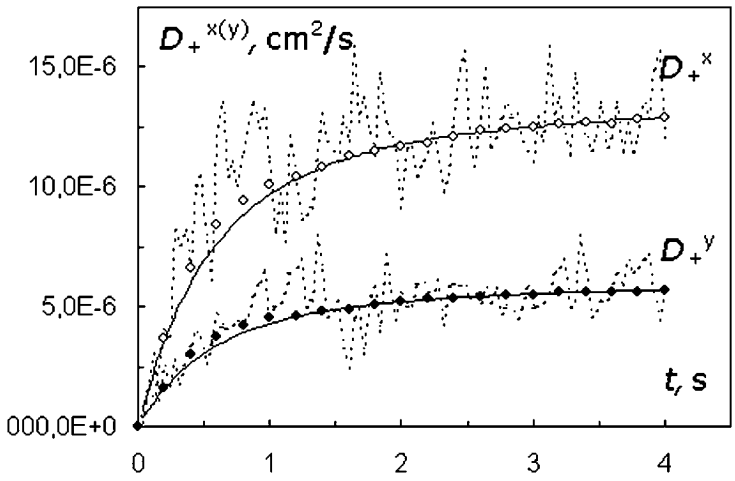

Figure 9. Time dependences of the diffusion coefficients D_p^x and D_p^y (dashed curves) measured in one experiment in the regions (x = 7–8 mm, y = 0–8 mm) and (y = 5–6 mm, x = 0–9 mm), respectively, and the values of $D_p^{x(y)}$ averaged over several experiments (●, ○) and their fits by formula (7) (solid curves).

The time dependence of the self-diffusion coefficient for non-interacting grains can be represented as [18]

$$D_p^{x(y)}(t) = D_0^{x(y)}\{1 - (1 - \exp(-\nu_{fr}t))/\nu_{fr}t\}. \quad (5)$$

Using the measurements of $D_p^{x(y)}(t)$ we can restore both the friction coefficient ν_{fr} and the diffusion coefficient $D_0^{x(y)} = D_p^{x(y)}$ ($t \to \infty$). The approximation of the experimental $D_p^{x(y)}(t)$ dependences by equation (5) for $T_+^x \cong 51$ eV and $T_+^y \cong 22$ eV (see figure 9) gives $\nu_+ = 3.1$ s^{-1},

$D_0^x \cong 1.4 \times 10^{-5}$ cm^2 s^{-1} and $D_0^y \cong 6.2 \times 10^{-6}$ cm^2 s^{-1}. It can easily be seen that the measured behaviour of $D_p^{x(y)}(t)$ is in good agreement with equation (5) for non-interacting grains. Note that, for strongly correlated dust systems ($\Gamma_n > 40$–50), the time dependence of the diffusion coefficient D_p is nonmonotonic; in contrast to the experimental data shown in figure 9, it has a pronounced maximum [18].

4.3. Charge of dust grains

Photoemission charging plays an important role when irradiating grains with photons with energy $h\nu$ exceeding the photoelectron work function from the grain surface. The number of emitted electrons (the photocurrent) is proportional to the intensity of the incident radiation. The maximum kinetic energy of photoelectrons $\mathcal{K}_{max} = h\nu - W$ increases linearly with the incident radiation frequency ν and does not depend on the radiation intensity. Thus, the maximum photoemission grain charge Z_{max} can be found by equating the surface potential $\phi_s = eZ_{max}/a_p$ to the quantity $\mathcal{K}_{max}/e$ [14]:

$$Z_{max} = \{h\nu_{max} - W\}a_p/e^2, \tag{6}$$

where $h\nu_{max}$ is the maximum photon energy, which, in our case, is determined by the transmission function of the experimental chamber and corresponds to the wavelength $\lambda_{min} \cong 0.35$ μm [6]. Thus, for $\langle a_p \rangle = 37.5$ μm, we have $Z_{max} \approx 53\,000$. Generally, the photoelectron flux depends on the radiation source properties, the efficiency of radiation absorption Q, the quantum yield Y, and the temperature T_{pe} of the emitted electrons. Moreover, the grain charge is affected by the emission properties of grains and the presence of photoelectrons that return to the grain surface. The latter effect can significantly decrease the equilibrium grain charge Z_p compared to its limiting value Z_{max} [14].

Let us evaluate the charge of bronze grains exposed to solar radiation. To calculate the photon flux J, the solar radiation can be considered as blackbody radiation with the temperature $T_c = 5800$ K [13]:

$$J = \int_{\lambda_{min}}^{\lambda_0} f_{tr} c_1 \lambda^{-4} / [\{\exp(c_2/\lambda T_c) - 1\} hc] \, d\lambda, \tag{7}$$

where $\lambda_{min} \approx 0.35$ μm, λ_0 is the boundary wavelength for the photoelectric effect, and f_{tr} is the transmission function of the experimental windows (the uviol window of the ampoule and the quartz window of the Mir space station). We can take $f_{tr} \approx 0.85$ with good accuracy for our estimation of Z_p [6]. Thus, we have $J \approx 3.4 \times 10^{17}$ photon s^{-1} cm^{-2}. Since photons with energies of $\leq$4 eV are incapable of ionizing the buffer gas, the positive grain potential will be determined by the balance between electron recombination on the grain surface and the flux of the emitted photoelectrons.

Let us estimate the minimal value of particle charge Z_p, assuming that the system is non-opaque to the emitted electrons (all emitted electrons are trapped within the grain cloud). Then the electron density n_e in a dust cloud will obey the quasineutrality condition $n_e = Z_p n_p$. Here it should be emphasized that in our case the induced radiation ($\lambda < \lambda_{min} = 0.35$ μm) cannot ionize a noble gas, such as neon, with the ionization potential $I > 4$ eV. Thus, the considered system will consist of the positively charged dust grains and emitted electrons only. When the electron mean free path l_{ne} in collisions with neutrals is comparable with or exceeds the grain radius a_p ($l_{ne} > a_p$) the electron balance equation can be written in the form [25, 26]

$$Z_p n_p \left(\frac{8T_e}{\pi m_e}\right)^{1/2} = JY \exp\left(\frac{h\nu - W - e\phi_s}{T_{pe}}\right) \approx JY^* \frac{T_{pe}}{h\nu_{max} - W} \exp\left(\frac{h\nu_{max} - W - e\phi_s}{T_{pe}}\right), \tag{8}$$

where m_e is the electron mass, T_e is the plasma electron temperature, and Y^* is the mean quantum yield of caesium-coated bronze in the spectral range under study. The temperature T_{pe} of the photoemission electrons depends on the grain material and, in most cases, lies in the range 1–2 eV [12, 13]. Then, under the assumption $T_e \approx T_{pe} = 1.5$ eV, we obtain from equation (8) that, for the grain radius $\langle a_p \rangle = 37.5$ μm, the limiting charge $Z_{max} \approx 53\,000$ is attained at densities $n_p \approx 400$–200 cm^{-3} (which corresponds to $Y^* \approx (0.8\text{–}4) \times 10^{-2}$, depending on the thickness of the caesium layer and its chemical purity). Thus, at $n_p < 400$ cm^{-3}, the electrons returning to the grain surface will not significantly affect the equilibrium grain charge. The higher n_p, the lower the equilibrium charge; thus, at $n_p \approx 900$ cm^{-3} ($Y^* \approx 8 \times 10^{-3}$), we have $Z_p \approx 40\,000$.

The electron temperature in the system under study may be different from the temperature T_{pe} of the photoelectrons leaving the grain surface. Thus, in the absence of an electric field, the characteristic time of electron energy relaxation (the time during which the electron energy falls by a factor of $\sim$2.7) is determined as $\tau_u \approx \tau\delta^{-1}$, (where $\tau = \nu_{ne}^{-1}$, is the electron–neutral collision frequency, and δ^{-1} is the number of effective collisions for electron–neutral energy transfer) and the effective relaxation length is $\Lambda_u \approx l_{ne}\delta^{-1/2}$ [15]. For neon, $\delta \approx 10^{-4}$ and, the relaxation length is Λ_u (cm Torr^{-1}) $\approx 12/P$. At the given pressure, this length is $\sim$0.3 cm; i.e., it is longer than the mean distance $l_p \sim 0.15$–0.18 cm between the dust grains, which are the source of background electrons. Hence, the emitted electrons lose about 30% of their initial energy over a distance of $\sim l_p/2$. Such an insignificant energy loss can readily be balanced by the stochastic energy input due to the presence of electric fields in the system [15]. Accordingly, in further calculations, we assume that $T_{pe} \cong T_e$.

The theoretical estimates of Z_p by formulae (6) and (8) can only provide the order of magnitude of the photoemission charge acquired by a grain because they strongly depend on the accuracy with which the grain parameters (work function W and quantum yield Y) and the spectrum of inducing radiation are determined; in turn, this accuracy depends on the specific experimental conditions. To measure the charges of individual grains moving with velocity V in a known electric field E, one can use the equation of motion [6]

$$dV/dt = -\nu_{fr} V + EeZ_p/m_p. \tag{9}$$

To solve equation (9), one needs *a priori* data on the electric field E, which (as well as theoretical estimates of the grain charge) depends on the transparency of the dust cloud to the emitted photoelectrons. Let us suppose that, at $t > 100$ s, all the emitted electrons have already left the dust cloud and the electric field E is equal to the field of a uniformly charged cylinder: $E \approx 2\pi e Z_p n_p x_R$ where x_R is the distance from the tube axis. In this case, estimating the grain charge from equation (9) with the use of the measured values of dV/dt and V for individual grains [6] gives charges ranging from $Z_p \approx 4 \times 10^4$ ($\nu_{fr} = 3$ s^{-1}) to $Z_p \approx 3 \times 10^4$ ($\nu_{fr} = 4$ s^{-1}), depending on the chosen value of the friction coefficient ν_{fr}.

In a cloud transparent to photoelectrons ($n_e = 0$), the grain charge Z_p can also be evaluated from the measured time dependence of the grain density $n_p(t)$, which characterizes the rate with which like-charged dust grains escape from the measurement volume due to electrostatic

repulsion. If the electric forces acting on an individual grain from all the other grains are balanced by the friction forces, then the dependence $n_p(t)$ can be approximated as [6]

$$n_p(\Delta t) = n_p^{t_0}(1 + 3\omega_0^2 \Delta t/\nu_{fr})^{-1} \tag{10}$$

where $\omega_0 = eZ_p\{n_p^{t_0}/m_p\}^{1/2}$, a $n_p^{t_0}$ is the dust grain density at a certain time $t = t_0$, and $\Delta t = (t - t_0)$. Approximation (10) allows one to determine ω_0 by fitting the calculated results to the experimental data; the result obtained makes it possible to find the grain charge. Figure 6 presents the results of approximating the experimental data by equation (10) under the assumption that the system becomes transparent as the grain density decreased to values lower than $n(t) = 90$ cm^{-3} ($t > 45$ s) and $n_p^{t_0} \equiv n_p$ ($t_0 = 45$ s). Hence, it follows that $3\omega_0^2/\nu_{fr} \approx 0.007$ s^{-1} for $n_p^0 = 195$ cm^{-3} and $n_p^{t_0} = 0.37 n_p^0$ and that $3\omega_0^2/\nu_{fr} \approx 0.01$ s^{-1} for $n_p^0 = 300$ cm^{-3} and $n_p^{t_0} = 0.3 n_p^0$. Therefore, the grain charge is $Z_p = (4.3 \pm 0.2) \times 10^4$ at $\nu_{fr} \approx 3$ s^{-1}. At $\nu_{fr} \approx 4$ s^{-1} Z_p is larger by ~15%.

Figure 6 also presents the results of calculations of $n_p(t)/n_p^0$ using molecular dynamics for the parameters close to the experimental ones under the assumption that the system is transparent to the emitted electrons. A set of three-dimensional equations of motion was solved for a cylindrical ampoule (see figure 2) with the random (Langevin) force F_{br}, assuming that the grains have zero initial velocities and are absorbed on the cylinder wall:

$$m_p \frac{d^2\vec{r}_k}{dt^2} = \sum_j \Phi(r)|_{r=|\vec{r}_k - \vec{r}_j|} \frac{\vec{r}_k - \vec{r}_j}{|\vec{r}_k - \vec{r}_j|} - m_p \nu_{fr} \frac{d\vec{r}_k}{dt} + \vec{F}_{br}. \tag{11}$$

Here, $\Phi(r) \approx (eZ)^2/r^2$, and r is the distance between the two interacting grains. It can easily be seen that the assumption of system transparency (Coulomb repulsion) allows one to describe the experimental data within the applicability range of formula (10) for $t > 45$ s. At $t < 20$ s, the rate at which grains escape from the measurement volume is significantly lower. This effect manifests itself in the magnitude of the recorded drift velocities of dust grains, which are lower than those expected for a transparent cloud: $V \approx 2\pi(eZ_p)^2 n_p x_R/(\nu_{fr} m_p)$ (see equation (9)). The estimated minimum drift velocity $V \approx (0.1\ \text{s}^{-1} x_R)$ for this case is shown in figure 7(a) by the dashed-and-dotted curve for $Z_p = 4.3 \times 10^4$ and $n_p = 200$ cm^{-3}. This phenomenon can be related to the presence of the polarization electric field, whose magnitude is lower than the electric field in a transparent system of charged grains by a factor of $\sim(\lambda/R)^2$, where λ is the electron Debye radius [15] ($\lambda^2 = T_e/4\pi e^2 n$). The possibility of polarization caused by the separation of opposite charges is determined by the requirement that the dust cloud is opaque to the emitted electrons (see the last section for details).

In a two-component system consisting of grains and electrons, the approximation of the dust cloud opacity corresponds to the quasineutrality condition

$$\delta n = |n_e - n_p| \ll n \approx n_e \approx Z_p n_p.$$

For a cylinder of radius R, this is true when [15]

$$\delta n/n \approx (\lambda/R)^2 \ll 1. \tag{12}$$

Thus, for a dust cloud in a 1.5 cm radius tube, condition (10) is met at $n_e \approx Z_p n_p \gg (2.5\text{–}4.9) \times 10^5$ cm^{-3} (for $T_e \cong 1\text{–}2$ eV)

The other limiting case is that where all the emitted electrons freely escape from the system ($n_e \approx 0$):

$$e\Delta\varphi \leq T_e,$$

where $\Delta\varphi = \pi Z_p n_p R^2$ is the potential difference in the electric field of a uniformly charged cylinder of radius R. Hence, the criterion for the dust cloud to be transparent to photoelectrons can be obtained from the condition

$$\lambda_p/R > 0.5 \tag{13}$$

where $\lambda_p^2 = T_e/(4\pi e^2 Z_p n_p)$ is a quantity equivalent to the Debye radius squared of an opaque system. Thus, the condition that the system is transparent to the emitted electrons is determined by the parameter λ/R, where $\lambda^2 = T_e/(4\pi e^2 Z_p n_p)$ both in the case of $n_e \approx Z n_p$ (when this quantity can be associated with the screening length in a two-component system) and at $n_e \approx 0$. The experimental time dependence of λ/R is shown in figure 6 for the grain parameters (Z_p, n_p) measured at $T_e = 2$ eV. Here, the dashed-and-dotted curves show the margins $\lambda/R = 0.5$ and $\lambda/R = 0.33$ corresponding to the limiting cases of transparent and opaque dust clouds (see equations (12) and (13)). It can be seen that the region $\lambda/R > 0.5$, in which the system can be assumed to be transparent ($t > 60$ s), approximately corresponds to the time domain in which the grain charges were measured using this assumption.

4.4. Characteristic times for different dynamic regimes

The data on the grain charges and friction coefficients allow us to estimate the characteristic times and frequencies in a dusty system for different dynamic regimes. In the case of the dust plasma frequency $\omega_p = Z_p e(4\pi n_p/m_p)^{1/2}$ less than the friction coefficient ν_{fr}, the time τ_{Maxw} during which dynamic equilibrium in a system of charged grains is established is determined by [6, 15]

$$\tau_{Maxw} \cong \nu_{fr}/\omega_p^2. \tag{14}$$

At $n_p = 195$–300 cm^{-3}, we have $\tau_{Maxw} \sim 4$–6 s, which is close to the relaxation times for the temperature and intergrain correlation observed in our experiments (see section 4.1). The minimum value of the coupling parameter Γ_n^{min} in the state of dynamic equilibrium can be estimated by choosing the maximum temperature $T_p \equiv T_x = 51$ eV and the minimum grain density $n_p^0 = 195$ cm^{-3}. Since in our experiments $\kappa < 0.5$ ($T_e = 1$–2 eV), we have $\Gamma_n \equiv (1 + \kappa + \kappa^2/2)\exp(-\kappa)\Gamma \cong \Gamma \equiv (eZ_p)^2/l_p T_p$. Consequently, at $Z_p \approx 4.3 \times 10^4$ ($\nu_{fr} = 3$ s^{-1}), we have $\Gamma_n^{min} \approx 32$.

In the experiments performed under solar irradiation (see section 4.1, second stage of the experiment), the time τ_{Maxw} during which the dynamic equilibrium in a dusty system is established can be measured by monitoring the decay of the initial grain velocity $V(t)$ acquired with shaking the ampoule. This velocity should behave as $\sim\exp(-t/\tau_{Maxw})$ [15]. The approximation of the $V(t)$ dependence by the curves $V(t) = V(0)\exp(-t/\tau_{Maxw})$ at $\tau_{Maxw} \cong 1$ s is shown in figure 3. The obtained value of τ_{Maxw} is in excellent agreement with a value of $\sim$1 s, calculated by equation (14) for the measured parameters: $n_p \approx 900$ cm^{-3}, $Z_p \approx 4.3 \times 10^4$, $\nu_{fr} = 3$ s^{-1}.

We note that the high-frequency $\omega \sim 4.5$–5.2 s^{-1} dust grain oscillations (see figure 3) during the relaxation to dynamic equilibrium could also be due to the polarization effects related to the separation of opposite charges. Thus, for charged-particle oscillations with frequency ω and amplitude A, that is, close to one-half of the characteristic spatial scale for charge separation ($2A = \lambda$) in the polarization electric field (which is proportional to $\sim T_e$), we can write $m_p(\omega\lambda/2)^2/2 \approx 4\pi e^2 Z_p^2 n_p \lambda^2 \equiv Z_p T_e$. Hence, at $n_p \approx 900$ cm^{-3} and $Z_p \approx 4.3 \times 10^4$, the oscillation frequency is $\omega = eZ_p\,(32\pi n_p/m_p)^{1/2} \approx 4.6$ s^{-1}. One can easily see that the obtained

frequency ω is higher by $\sqrt{8} \sim 3$ times than the dust frequency ω_p, because we use the value of $A = \lambda/2$ (instead of λ which is true for half-infinitive systems) as the characteristic scale for charge separation. Under assumption $A = \lambda$ the polarization effects near the opposite ampoule wall would not be taken into consideration.

4.5. Ambipolar diffusion

Let us consider a two-component system consisting of positively charged grains and the photoelectrons emitted by them. Because of a significant difference in the electron mobility μ_e and the dust grain mobility μ_p, the components of this system will be separated in the entire ampoule volume and a negative surface charge will arise on the wall. The arising polarization electric field will impede the further separation of the charged components; consequently, the electrons will diffuse together with heavy grains with a certain effective coefficient of ambipolar diffusion D_a. The D_a value is determined by the diffusion coefficient of the less-mobile component; in the absence of external magnetic and electric fields, it can be written as [15]

$$D_a = \{D_e\mu_p + D_0\mu_e\}/\{\mu_+ + \mu_e\}, \tag{15}$$

where D_e is the coefficient of free diffusion,

$$D_e = T_e/\nu_{en}m_e, \tag{16}$$

and D_0 is given by formula (3). Since $\mu_e \gg \mu_p$, the coefficient of ambipolar diffusion can be written as $D_a \approx D_0 + D_e\mu_p/\mu_e$. Then, with allowance for formulae (3) and (16), we have

$$D_a \approx (1 + Z_pT_e/T_p)D_0. \tag{17}$$

We note that equations (15)–(17) are valid only in the case of a weakly ionized electron–dust system, in which dissipation is determined by the buffer gas neutrals, whereas the collisions between charged particles are unimportant. On the other hand, the coefficient of ambipolar diffusion describes the polarization effects, which are absent in a rarified plasma with low densities of charged components. In such a plasma, particle diffusion is determined by coefficients (3) and (16). Diffusion is ambipolar when the plasma is quasineutral and condition (12) is met. Hence, the regime of ambipolar diffusion is determined by the inequality $\lambda/R < 0.33$ ($\delta n/n_e < 10$). Thus, for $t < 10$ s (figure 6), the polarization effects related to the separation of opposite charges are feasible in the system under study.

Assuming that, at $t < 10$ s, the charge loss in our experiment is related to the ambipolar diffusion toward the wall, the mean diffusion loss rate for dust grains can be written as [15]

$$dn_p/dt = -n_p\nu_d, \tag{18}$$

where ν_d is the effective diffusion loss rate,

$$\nu_d \equiv -D_a/\Lambda_d^2, \tag{19}$$

and Λ_d is a characteristic scale length. For a cylinder of radius $R = 1.5$ cm and length $L = 4R$, we have $\Lambda_d^2 \approx ((2.4/R)^2 + (\pi/L)^2)^{-1} = 0.75$ cm [15]. The diffusion loss rate ν_d can be estimated by the rate at which the relative grain density changes. The experimental curve $n_p(t)/n_p^0$ is in good agreement with the exponential solution $n_p = n_p^0\exp(-\nu_d t)$ of equation (19) with $c\nu_d = 0.035$ s^{-1} at $t < 10$ s (see figure 6). Hence, the estimated

coefficient of ambipolar diffusion is $D_a = \Lambda^2 \nu_d \cong 1.3 \times 10^{-2}$ cm s^{-1}, which is much larger than the measured coefficients $D_0^{x(y)}$ of grain self-diffusion. To compare the obtained coefficient D_a with its theoretical value $D_a \approx Z_p T_e D_p / T_p$, we use the measured values $Z_p \approx (4.3 \pm 0.2) \times 10^4$ and $D_p/T_p \approx 2.8 \times 10^{-7}$ cm^2 s^{-1} eV^{-1} and assume $T_e = 1$–2 eV. Then, we have $D_a \approx (1.2$–$2.4) \times 10^{-2}$ cm^{-2} s^{-1}, which agrees with the coefficient of ambipolar diffusion measured by the rate at which the grains depart to the wall to within the accuracy in determining the characteristic length Λ_d, the grain parameters and the validity of the assumption $T_e = 1$–2 eV.

5. Conclusion

We have presented the experimental results on the dynamics of dust grains charged via photoemission under microgravity conditions. The velocity distribution, temperature, mean charge, and diffusion coefficient of the dust grains are determined. An analysis of the experimental data shows that, in the initial stage ($t < 10$ s), the particles undergo ambipolar diffusion; i.e., the densities of the charges of both signs are so high that the charge separation leads to the formation of a significant space charge, which induces the polarization electric field. The polarization caused by the separation of opposite charges decreases the drift velocities of the dust grains with respect to their velocities in a system transparent to photoelectrons and affects the excitation of high-frequency oscillations observed after the dynamic action on a dust system exposed to solar radiation. We emphasize that direct experimental observations of the phenomena related to charge separation in an electron–dust plasma are impossible under the Earth's gravity conditions because of the necessity of using an electric trap for levitation of dust particles in the gravity field.

To conclude, the experiments show that the interaction between dust grains hardly affects either the grain self-diffusion coefficient, which remains close to the Brownian one D_0, or ambipolar dust transfer, whose theory is based on neglecting Coulomb collisions between oppositely charged particles. Thus, we can suggest that, if the coupling parameter Γ is no higher than 30–35, then the transport properties of strongly dissipative systems of dust grains ($\omega_p/\nu_{fr} < 1$) with a weak screening of the grain charges ($\kappa < 1$) can be described with good accuracy in the gas dynamics approximation.

Acknowledgments

We are grateful to pilot-cosmonauts Pavel Vinogradov and Anatoly Solov'ev for carrying out the experiment on board the Mir space station. This study was supported in part by the Russian Foundation for Basic Research (project No 01-02-16658 and No 03-02-17240) and INTAS (grant No 2001-0319 and No 2000-0522).

References

[1] Thomas H *et al* 1994 *Phys. Rev. Lett.* **73** 652
[2] Melzer A, Trottenberg T and Piel A 1994 *Phys. Lett.* A **191** 301
[3] Zhakhovskii V V *et al* 1997 *J. Theor. Exp. Phys. Lett.* **66** 419
[4] Nunomura S, Misawa T, Ohno N and Takamura S 1999 *Phys. Rev. Lett.* **83** 1970
[5] Vaulina O *et al* 1999 *Phys. Rev.* E **60** 5959
[6] Fortov V E *et al* 1998 *J. Theor. Exp. Phys.* **87** 1087
[7] Vaulina O S *et al* 2002 *Phys. Rev. Lett.* **88** 035001

[8] Nefedov A P *et al* 2001 *J. Theor. Exp. Phys.* **95** 673
[9] Morfill G *et al* 1999 *Phys. Rev. Lett.* **83** 1598
[10] Fortov V E *et al* 2003 *Phys. Rev. Lett.* at press
[11] Tsytovich V N 1997 *Usp. Fiz. Nauk* **167** 57
[12] Goertz C K 1997 *Geophys. Rev.* **27** 271
[13] Grilikhis V A, Orlov P P and Popov L B 1986 *Sun Energy and Space Flights* (Moscow: Nauka)
[14] Rosenberg M, Mendis D A and Sheehan D P 1996 *IEEE Trans. Plasma Sci.* **24** 1422
[15] Raizer Y P 1991 *Gas Discharge Physics* (Berlin: Springer) (1987 (Moscow: Nauka) (in Russian))
[16] Cummins H Z and Pike E R 1974 *Photon Correlation and Light Beating Spectroscopy* (New York: Plenum) (1978 (Moscow: Mir) (in Russian))
[17] Vaulina O S and Vladimirov S V 2002 *Plasma Phys.* **9** 835
[18] Vaulina O S and Khrapak S A 2001 *J. Theor. Exp. Phys.* **92** 228
[19] Vaulina O S, Nefedov A P, Petrov O F and Fortov V E 2000 *J. Theor. Exp. Phys.* **91** 1147
[20] Vaulina O S *et al* 1999 *Phys. Rev.* E **60** 5959
[21] Thomas H and Morfill G 1996 *Nature* **379** 806
[22] Melzer A, Homann A and Piel A 1996 *Phys. Rev.* E **53** 2757
[23] Pieper J and Goree J 1996 *Phys. Rev. Lett.* **77** 3137
[24] Lifshitz E M and Pitaevskii L P 1981 *Physical Kinetics* (Oxford: Pergamon) (1979 (Moscow: Nauka) (in Russian))
[25] Sodha M S and Guha S 1971 *Adv. Plasma Phys.* **4** 219
[26] Samarian A A *et al* 2001 *Phys. Rev.* E **64** 6407